Materials Science-Poland, Vol. 23, No. 4, 2005

Characterization and EPR studies of TiC and TiN ceramics at room temperature

T. BODZIONY[1], N. GUSKOS[1, 2], A. BIEDUNKIEWICZ[3], J. TYPEK[1*], R. WRÓBEL[4], M. MARYNIAK[1]

[1]Institute of Physics, Szczecin University of Technology, al. Piastów 17, 70-310 Szczecin, Poland

[2]Solid State Section, Department of Physics, University of Athens, Panepistimiopolis, 15 784 Zografos, Athens, Greece

[3]Institute of Material Engineering, Szczecin University of Technology, al. Piastów 19, 70-310 Szczecin, Poland

[4]Department of Chemical and Environment Engineering, Szczecin University of Technology, Pułaskiego 10, 70-322 Szczecin, Poland

Four samples, namely TiC/C, TiN/C, (TiC + Fe_xC_y + Fe)/C and TiN/amorphous carbon, have been prepared and investigated. In the former three samples titanium compounds were placed in a carbon matrix, while in the fourth one TiN was surrounded by an amorphous carbon. The samples have been characterized by XRD, SEM, and electron diffraction spectroscopy. The crystallite sizes and lattice parameters of TiC and TiN have been determined by the X-ray diffraction method. XRD measurements have shown that the lattice constants of nanosized samples were smaller than those of microsized samples. An essential influence of the carbon matrix during the crystallization process on the lattice parameters and grain size was observed. Electron paramagnetic resonance (EPR) measurements of the samples were carried out at room temperature. A narrow EPR absorption line has been recorded for the TiC/C, TiN/C, and TiN/amorphous carbon samples, whereas for the (TiC + Fe_xC_y + Fe)/C sample a ferromagnetic resonance spectrum, mainly of α-Fe and cementite Fe_3C, has been recorded. The narrow resonance EPR line is explained by carrier motion – free electrons in the case of the TiN/C sample and holes (carbon vacancies) in the case of TiC/C and TiN/amorphous carbon samples – which could lead to the creation of the pseudogap state in TiC_x or TiN_x compounds.

Key words: *EPR; titanium carbide; titanium nitride*

1. Introduction

Nanomaterials, due to their enhanced physical properties, are attractive for various applications. For example, titanium carbide (TiC) and titanium nitride (TiN) possess

*Corresponding author, e-mail: typjan@ps.pl

many useful properties: extreme hardness, high strength, resistance to heat, corrosion and wear, high resistance to chemical attack, high thermal stability, good electrical and thermal conductivity, interesting magnetic properties and, in the case of TiN – an attractive golden colour [1]. Nanometer-sized magnetic materials have attracted attention of many researchers because they exhibit such unusual chemical and physical properties as superparamagnetism and quantum tunnelling of magnetization [2]. Nanocrystalline TiC and TiN can be synthesized by several methods, such as synthesis in the gas phase, synthesis based on carbothermal reduction in vapour–solid or vapour–liquid phases, sol-gel methods and mechanical processing [1].

The electric and magnetic properties of nonporous carbon systems are expected to be similar to those of nanohorns and/or nanotubes, because the main part of nanoporous carbon systems and nanohorn and/or nanotube samples is a quasiamorphous net of randomly oriented graphene fragments a few nanometers in size [3]. Electron paramagnetic resonance is a powerful and sensitive method for characterizing paramagnetic centres and ions, e.g. $Ti^{3+,}$ and is useful in studying disordered titanium carbide or titanium nitrite materials, in which an undesirable but possible inclusion of impurities into the sample should be taken into account.

2. Experimental

A nonhydrolytic sol-gel process has been applied for the preparation of TiC and TiN nanocrystals [1]. In the present work, mixtures of polyacrylonitryle, dimethylformamide and titanium chlorides were used to form gels containing Ti–C bonds and being precursors for the synthesis of titanium carbide as well as titanium nitride. The dispersed phase of the gel is formed by polymerising polyacrylonitryle crosslinked with titanium chlorides, which initially forms connections with the polymer chains as a result of intermolecular interactions and chemical bonds. Dimethylformamide acts as the dispersing agent in this system. All the operations and gel precursor preparations were carried out in a glove box under a protective atmosphere of argon using the Schlenk technique. The gel samples were heated in a furnace in inert and/or reactive atmospheres, depending on the desired products. The heating was carried out in a gas atmosphere, which contained argon and/or nitrogen, hydrogen and ammonia, under atmospheric pressure and in the temperature range of 293–1273 K. The reactions leading to the appearance of TiC and TiN phases proceeded at temperatures below 800 K. The parameters for manufacturing TiC and TiN phases with or without carbon as coatings and powders are subject to patenting procedure.

The following techniques were applied for sample characterization: scanning electron microscopy (JEOL JSM 6100), X-ray diffraction (PHILIPS X'PERT), transmission electron microscopy, and electron diffraction (JEOL JEM 1200EX). The obtained TiC/C and TiN powders, Ti–C coatings, and TiN/C pumice were additionally

characterized by microanalysis with wavelength dispersive and energy dispersive spectroscopy (IBEX System Noran Instruments and an Oxford ISIS 300).

EPR measurements were carried out with a conventional X-band (ν = 9.43 GHz) Bruker E 500 spectrometer, with 100 kHz magnetic field modulation. Prior to the measurements, the samples were magnetized by a steady magnetic field of 1.4 T to saturate any domain structure. All EPR measurements were performed at room temperature.

3. Results and discussion

Four ceramic samples, namely TiC/C, TiN/C, (TiC + Fe_xC_y + Fe)/C, and TiN/amorphous carbon have been prepared with sizes in the micrometer and nanometer scales. The titanium phases in three of them – TiC, TiN and (TiC + Fe_xC_y + Fe) – were surrounded by carbon (C), and by amorphous carbon in the fourth one (TiN). In comparison to the case of conventional high-temperature synthesis, we managed to lower the temperature of TiC and TiN synthesis, and achieved unique microstructural properties of the samples.

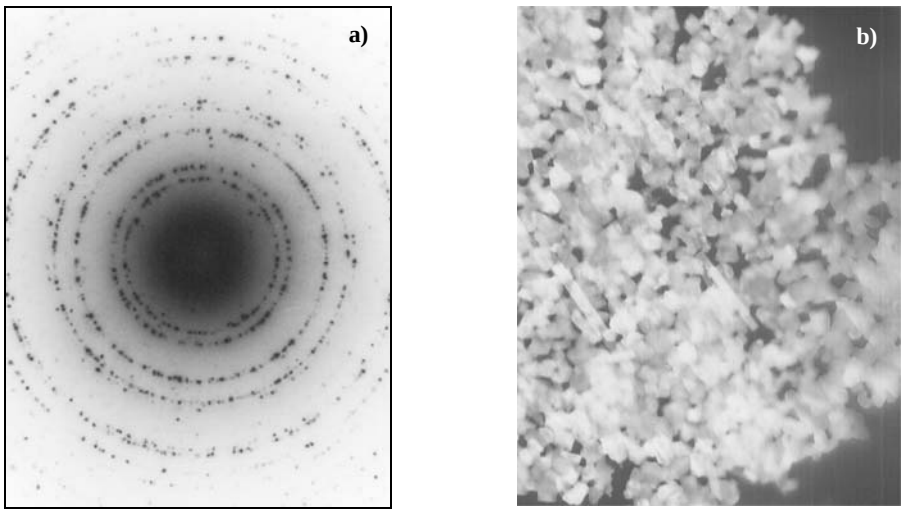

Fig. 1. TiC/C sample: electron diffraction pattern (a) and transmission electron micrograph (b)

The Transmission Electron Micrograph (TEM) and electron diffraction pattern of the TiC/C composite powder are presented in Figures 1a, b. Microscopic and microanalysis results suggest that the TiC phase is homogeneously dispersed in the carbon matrix. Figures 2a, b show the TEM image and electron diffraction pattern of the TiN/C composite powder. These TEM images show that the powder contains two crystalline phases: graphite and titanium carbide or titanium nitride, respectively. TEM investigations of the TiC/C and TiN/C particles showed that they formed with

an average size below 100 nm and 50 nm, respectively. Figures 3a, b show the TEM image and electron diffraction pattern of the TiN/amorphous carbon composite powder. The X-Ray powder diagrams of TiC/C (1), TiN/amorphous carbon (2), and TiN/C (3) are presented in Figure 4.

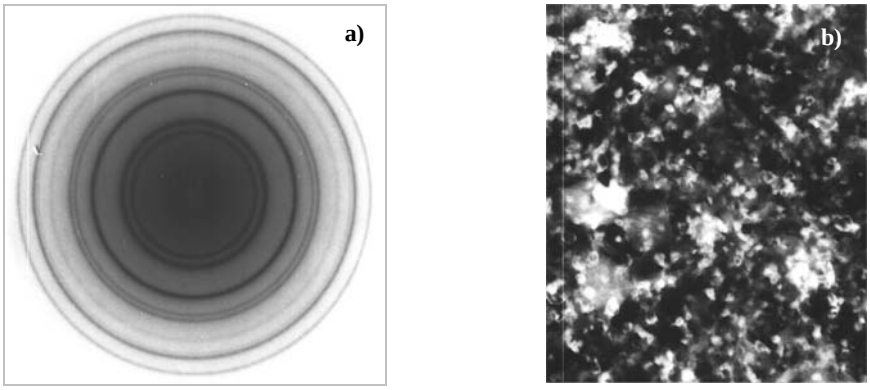

Fig. 2. TiN/C sample: electron diffraction pattern at room temperature (a) and transmission electron micrograph (b)

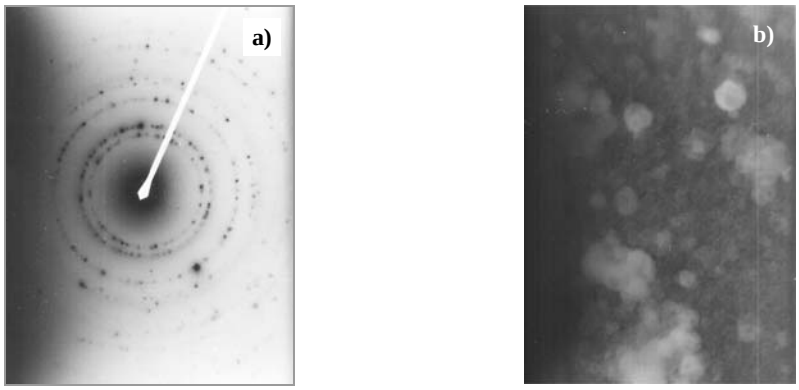

Fig. 3. TiN/amorphous carbon sample: electron diffraction pattern at room temperature (a) and transmission electron micrograph (b)

The lattice constants and crystallite sizes of the prepared composite powders have been determined using an X-ray diffraction method [4] and are shown in Table 1. The lattice constant of TiN is 0.4242 nm according to the 38-1420 ICDD (International Center of Diffraction Data) card. The lattice constant of TiN/amorphous carbon nanoparticles is practically the same as that from the ICDD card (only 0.1% less), while the lattice constant of TiN/C is significantly smaller (by about 1.1 %). The most important difference in the lattice constant was found for the TiC/C sample. The lattice constant of TiC is 0.4327 nm according to the 32-1383 ICDD card, and the lattice constant of TiC/C nanoparticles is 2.3 % smaller than for micrometer-sized TiC. Note

that the TiN/C and TiC/C samples, for which a significant difference in the lattice constant is observed, have small crystallite sizes. A comparison of the lattice parameters and grain sizes of TiN and TiC suggests an essential influence of the presence of the carbon matrix during the crystallization process.

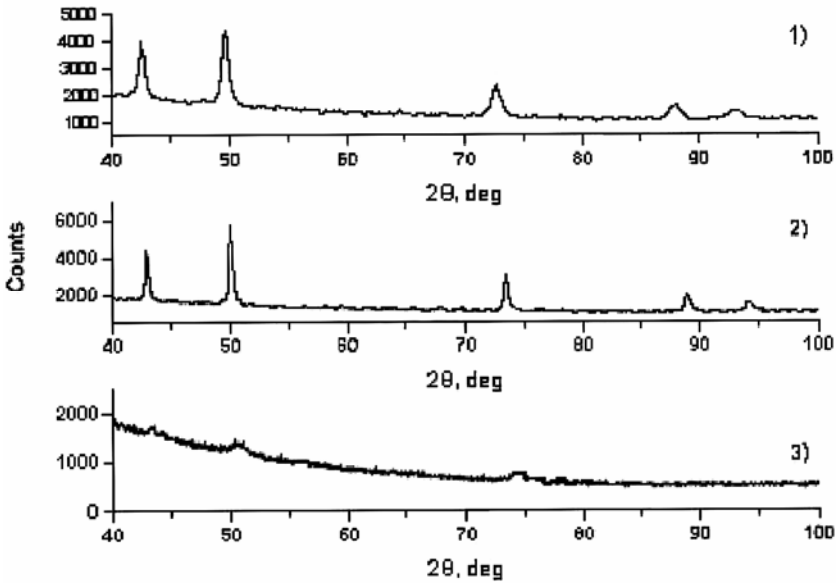

Fig. 4. XRD powder diagram of: 1 – TiC/C, 2 – TiN/amorphous carbon, 3 – TiN/C

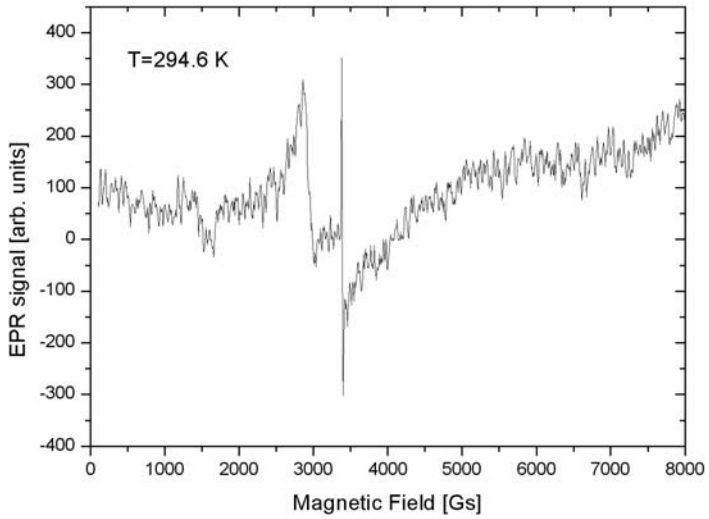

Fig. 5. The EPR spectrum of the TiC/C sample at room temperature

Table 1. The lattice constants of the TiN and TiC bulk compounds in the carbon matrix as compared to their values in the micrometer scale

Compound	Lattice constant [Å]	Lattice constant ratio [%]	Crystallite size [nm]
TiN/C	4.194(1) 4.242 (ICDD)	–1.1 Δa = 0.048 Å	8.3(9) >1000
TiN/amorphous carbon	4.238(1) 4.242 (ICDD)	–0.1 Δa = 0.004 Å	55.1(8) >1000
TiC/C	4.228(1) 4.327 (ICDD)	–2.3 Δa = 0.099 Å	12.3(6) >1000

Table 2. Values of the EPR parameters of TiN and TiC compounds in the carbon matrix

Compound	g	ΔB_{pp} [Gs]	Relative intensity
TiN/C	2.0025(3)	4.0(2)	1
TiN/amorphous carbon	1.9935(6)	82.0(5)	34
TiC/C	1.9959(3)	21.1(5)	2

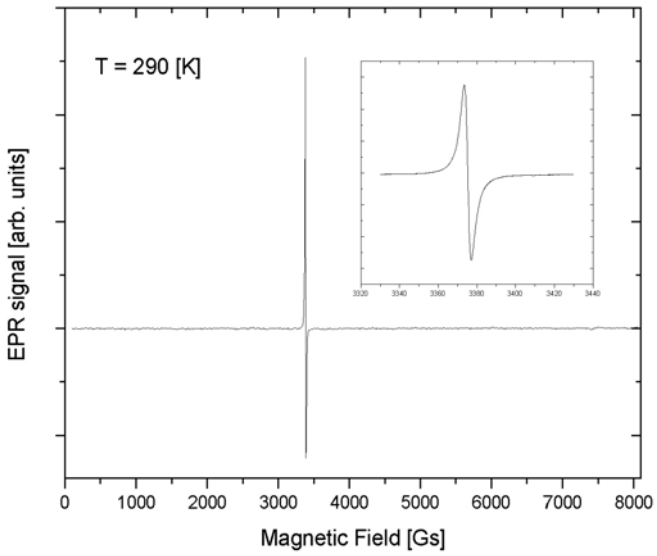

Fig. 6. The EPR spectrum of the TiN/C sample at room temperature. The inset in this picture shows the resonance line in an expanded magnetic field scale

Figure 5 shows the EPR spectrum of the TiC/C sample at room temperature. A sharp EPR line at a resonance field of B_{res} = 3385(9) Gs with a peak-to-peak linewidth of ΔB_{pp} = 21.0(5) Gs (see Table 2) can be observed. Another EPR line cantered at B_{res} = 2924(9) Gs is also visible. The EPR spectrum of the TiN/C sample at room temperature is presented in Figure 6. A characteristic feature of this spectrum is

a very high and sharp needle-like resonance line cantered at B_{res} = 3375(9) Gs with a linewidth of ΔB_{pp} = 4.0(2) Gs (see Table 2). The inset in this picture shows this line in an extended scale. This EPR resonance line is almost symmetrical. Figure 7 shows the EPR spectrum of the TiN/amorphous carbon sample at T = 297 K. A relatively wide resonance signal is obtained with the resonance field of B_{res} = 3378(9) Gs and a peak-to-peak linewidth of ΔB_{pp} = 82.0(5) Gs (Table 2). The narrowest resonance line is seen for the TiN/C sample, above five times smaller than in the case of TiC/C. In the amorphous carbon matrix, this resonance line is observed with a much larger linewidth (Table 2).

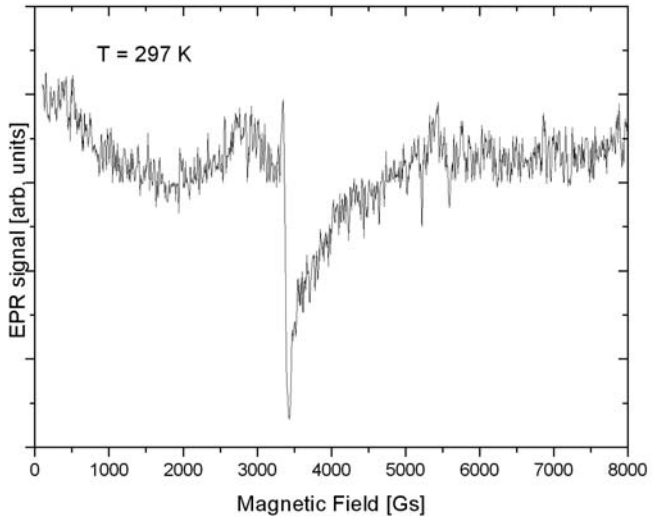

Fig. 7. The EPR spectrum of the TiN/amorphous carbon sample at room temperature

A resonance line with a different shape is presented in Figure 8, which shows the EPR spectrum of the (TiC + Fe_xC_y + Fe)/C sample at T = 307 K. In this figure, a very wide and strong EPR signal, shifted to low magnetic fields, is observed. Mossbauer spectroscopy for the (TiC + Fe_xC_y + Fe)/C sample has shown the presence of five forms of iron, mostly Fe^{3+}, α-Fe, and cementite (Fe_3C) [5]. We suggest that in ferro-magnetic resonance (FMR), the (TiC + Fe_xC_y + Fe)/C sample is observed, originating from α-Fe and cementite [6, 7].

A narrow EPR absorption line has been recorded for the three samples (TiC/C, TiN/C, TiN/amorphous carbon). In Table 2, the parameters of this signal – the g-parameter, peak-to-peak linewidth ΔB_{pp}, and integrated intensity – are presented for the three samples. The relative intensity is computed as a ratio of the EPR intensity of a given sample to the intensity of the weakest sample (TiN/C). It can be seen that the intensity of the TiC/C sample is two times larger, while the intensity of the TiN/amorphous carbon is 34 times larger than the intensity of the reference TiN/C sample. The g-parameter of TiN/C is almost equal to the g-value of free electrons

(2.0023), hence it appears that the narrow resonance line originates from free electrons. For TiN/amorphous carbon and TiC/C samples, the *g*-parameter is less than 2 and a resonance line is observed with a slightly asymmetric lineshape. In Ref. 8, the role of hole conductivity in EPR is stressed. We suggest that the narrow line in TiN/amorphous carbon and TiC/C samples is produced by hole movement [9], especially by the movement of carbon vacancies [10]. The conductance can include two types of current carrier movements: surface conductance across the percolating network of nanoclusters, and bulk conductance due to free carrier jumps through potential barriers at carbon cluster boundaries [8, 10].

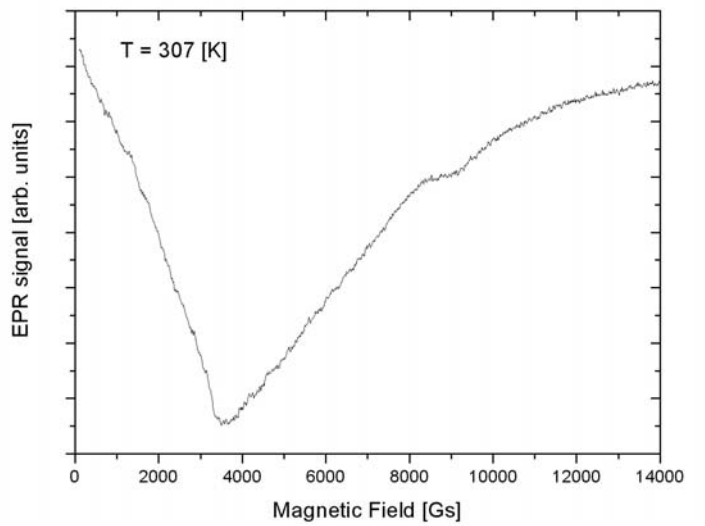

Fig. 8. The EPR spectrum of the (TiC + Fe_xC_y + Fe)/C sample at T = 307 K

For the TiC/C sample, an additional intense EPR line at higher resonance fields was recorded. It is suggested that this EPR spectrum could arise from complexes of Ti^{3+} ions [9]. The decrease in the lattice constants for nanometer-sized samples of crystallites could be the effect of titanium(III), and these ions could form centres of disorder, which might promote the semiconductor-metal transition at higher temperatures [11]. The shorter bonding between titanium(III) could bring about the disordered state more easily in the nanometer-sized TiC_x system than in titanium nitrites.

4. Conclusions

Four samples – TiC/C, TiN/C, (TiC + Fe_xC_y + Fe)/C, and TiN/amorphous carbon – have been prepared and investigated. These samples have been characterized by XRD, SEM, and electron diffraction spectroscopy. TiC and TiN crystallite sizes and lattice parameters have been determined by X-ray diffraction. XRD measurements

have shown that the lattice constants for nanometer-sized samples are smaller than for micrometer-sized ones. This fact is especially important for the physical properties (electrical and mechanical) of the TiC_x/C system. A comparison of the lattice parameters and grain sizes of TiN and TiC suggests an essential influence of the carbon matrix during crystallization process on their values. EPR measurements of the samples have been carried out at room temperature. Narrow EPR absorption lines were recorded for the TiC/C, TiN/C, and TiN/amorphous carbon samples, and essential differences were observed in the values of their EPR parameters. We suggest that the narrow resonance line originates from free electrons in the case of the TiN/C sample, and from hole movement (carbon vacancies) in the case of TiC/C and TiN/amorphous carbon samples, which could lead to the pseudogap in TiC_x or TiN_x compounds.

Acknowledgments

This work was partially supported by grant PBZ-KBN-095/TO8/2003.

References

[1] BIEDUNKIEWICZ A., Mater. Sci., 21 (2003), 445.
[2] TANGO T., HATSUTA T., MIYAJIMA K., KISHADA M., TASHIRO S., WAKABAYASHI K., J. Am. Ceram. Soc., 85 (2002), 2188.
[3] KYUTT R. N., SMORGONSKAYA E. A., DANISHEVSKII A. M., GORDEEV S. K., Solid State Phys. (in Russian), 41 (1999), 1359.
[4] BIEDUNKIEWICZ A., WROBEL R., submitted for publication in Mater. Sci.-Poland.
[5] Private communication, J. Suwalski, Institute for Nuclear Studies, Świerk, Poland.
[6] NARKIEWICZ U., GUSKOS N., ARABCZYK W., TYPEK J., BODZIONY T., KONICKI W., GASIOREK G., KUCHAREWICZ I., ANAGNOSTAKIS E.A., Carbon, 42 (2004), 1127.
[7] GUSKOS N., ANAGNOSTAKIS E. A., TYPEK J., GASIOREK G., BODZIONNY T., NARKIEWICZ U., ARABCZYK W., KONICKI W., Mol. Phys. Rep., 39 (2004), 58.
[8] SHANINA B. D. KONCHITIS A.A., KOLESNIK S.P., VEYNGER A.I., DANISHEVSKII A.M., POPOV V.V., GORDEEV S.V., GRECHINSKAYA A.V., Carbon, 41 (2003), 3027.
[9] VAN DOORSLAER S., SHANE J.J., STOLL S., SCHWEIGER A., KRANENBURG M., MEIER R.J., J. Organ. Chem., 634 (2001), 185.
[10] DYSON F.J., Phys. Rev., 98 (1955), 349.
[11] GUSKOS N., TYPEK J., BIEDUNKIEWICZ A., PATAPIS S., KARKAS K., MARYNIAK M., to be published in Rev. Adv. Mater. Sci. (2004).

Received 23 October 2004
Revised 24 February 2005